High-Speed 850 nm Quasi-Single-Mode VCSELs for Extended-Reach Optical Interconnects

Rashid Safaisini, Krzysztof Szczerba, Petter Westbergh, Erik Haglund, Benjamin Kögel, Johan S. Gustavsson, Magnus Karlsson, Peter Andrekson, and Anders Larsson

***Abstract*—This paper presents recent results on high-speed, quasi-single-mode, 850 nm vertical-cavity surface-emitting lasers (VCSELs) with a narrow spectral width for extended-reach optical interconnects. The top mirror reflectivity is adjusted for high output power, slope efficiency, and small signal modulation bandwidth. An oxide confined VCSEL with an ~3 μm aperture diameter delivers 2 mW of output power and reaches a resonance frequency as high as 25 GHz and a modulation bandwidth exceeding 20 GHz. A small K-factor of 0.17 ns and a large D-factor of 17.3 GHz/mA$^{1/2}$, extracted from the VCSEL modulation response, along with the improved DC and modal properties enable energy-efficient data transmission at high bit rates over long-distance multimode fiber. Error-free transmission at bit rates exceeding 20 Gbits/s over 1.1 km of OM4 fiber is demonstrated and shown to be limited mainly by the photoreceiver bandwidth. A theoretical investigation of the dependence of link performance on photoreceiver bandwidth is also presented.**

***Index Terms*—High-speed data communication; Long-distance data transmission; Multi-mode fiber; Narrow spectral width; Optical interconnect; Quasi-single-mode laser; Vertical-cavity surface-emitting laser (VCSEL).**

I. Introduction

The demand for high-speed optical data communication is perpetually growing in our modern Internet era because of the need for fast access to large amounts of information. This technology trend not only requires an increase of the link speed to 20–25 Gbits/s, but also an extension of the interconnect length up to 2 km for intrabuilding links in office areas and data centers [1,2]. Owing to their unique properties, vertical-cavity surface-emitting lasers (VCSELs) have already been a part of multiple standards and are widely deployed in applications, such as optical links and networks in data centers and high-performance computing systems [3,4]. The combination of 850 nm VCSELs and multimode fibers (MMFs) has been the best solution for short-reach high-speed optical interconnects for several years [4,5]. Even though single-mode fibers (SMFs) with long-wavelength lasers (1310 and 1550 nm) is a proven solution for >10 km links, MMF links at 850 nm are more cost efficient for extended short-reach interconnects (up to ~2 km) as a result of more tolerant optical alignment and lower cost optoelectronic components, assembly, and packaging, although the price per kilometer of MMFs is higher than for SMFs.

One of the main challenges of high-bit-rate transmission over long MMFs arises from the limited bandwidth caused by effects of chromatic dispersion (mainly due to material dispersion) and modal dispersion (depending on the fiber refractive index profile). However, in the new generations of MMFs, the chromatic dispersion can be compensated by modal dispersion by proper index profiling for a left-tilted differential mode delay specification [6]. With this technique, MMFs with an effective modal bandwidth exceeding 4700 MHz·km (OM4 fiber) have already been introduced to increase the reach of 10 Gb Ethernet from 300 to 550 m [7]. Moreover, improving VCSEL modal properties to reduce the number of transverse optical modes, and consequently the emission spectral width, is crucial for reducing the effects of chromatic dispersion and achieving even longer transmission distance [8]. In addition to improved modal properties, VCSELs utilized in high-bit-rate and long-reach applications should meet at least two more requirements: improved speed to increase the total bandwidth of the link and improved optical output power to overcome optical penalties and losses and reach the required received power for error-free detection. A compromise may need to be considered to reach the best performance for a particular bit rate and fiber length, since simultaneous achievement of all three requirements might be challenging.

Large efforts have been devoted to increasing the bit rate and/or the distance at error-free transmission (defined as bit error rate (BER) < 10^{-12}) over MMF using directly modulated 850 nm VCSELs [8–16]. Record bit rates of 47 Gbits/s back-to-back (BTB) and 44 Gbits/s over 50 m of MMF, using a VCSEL with a 27 GHz modulation bandwidth, were recently reported; these rates were obtained by

Manuscript received January 2, 2013; revised May 7, 2013; accepted May 10, 2013; published June 13, 2013 (Doc. ID 182555).

R. Safaisini (e-mail: rashid.safaisini@chalmers.se), K. Szczerba, P. Westbergh, E. Haglund, J. S. Gustavsson, M. Karlsson, P. Andrekson, and A. Larsson are with the Photonics Laboratory at the Department of Microtechnology and Nanoscience, Chalmers University of Technology, Göteborg 412 96, Sweden.

B. Kögel was with the Photonics Laboratory at the Department of Microtechnology and Nanoscience, Chalmers University of Technology, Göteborg 412 96, Sweden. He is now with Vertilas GmbH, Garching, Germany.

http://dx.doi.org/10.1364/JOCN.5.000686

reducing the mirror resistances and employing a short cavity for improved carrier transport and optical confinement [9]. Moreover, various attempts focused on increasing the transmission distance by utilizing narrow spectral width VCSELs, either by employing an integrated mode filter to suppress higher order modes or a small oxide aperture to support a smaller number of lasing modes. Data transmission over 500 m of MMF at 25 Gbits/s was reported, obtained by using a VCSEL with a 5 μm oxide aperture and an integrated mode filter [10] and also a VCSEL with ~3 μm oxide aperture [11]. Small-aperture VCSELs offer a less complex approach for the required modal properties and have proved to be more energy efficient than large aperture VCSELs, as investigated by a group at TU Berlin [12], due to improved dynamics related to their small cavity volume, although there might be some concerns about their reliability [17]. There have been reports of 25 Gbits/s transmission over 300 [13] and 603 m [14] of MMF using quasi-single-mode (side-mode suppression ratio (SMSR) ~20 dB) VCSELs with an ~3–4 μm aperture diameter. The highest bit rate achieved at longer distance is 20 Gbits/s over 1100 m, which was also accomplished using a small-aperture, quasi-single-mode VCSEL [15]. The highest bit-rate–distance product was reported in [16], where transmission at 10 Gbits/s over 2.8 km of high-bandwidth MMF was demonstrated using a single-mode VCSEL.

This paper presents results from our recent work on small-aperture, narrow-spectral-width, quasi-single-mode VCSELs with a modulation bandwidth exceeding 20 GHz. This has enabled transmission at bit rates exceeding 20 Gbits/s over more than 1 km of OM4 MMF with low energy dissipation. The top distributed Bragg reflector (DBR) reflectivity was reduced [18] for low damping of the modulation response, high slope efficiency, and high output power to meet requirements in terms of speed, modulation efficiency, and received optical power. To the best of the authors' knowledge, this represents the state of the art for transmission at high bit rates over more than 1 km of MMF using a directly modulated VCSEL.

II. VCSEL Design and Fabrication

A. Structure

The epitaxial structure is grown by metal-organic vapor phase epitaxy on an undoped GaAs substrate. The n-type (Si-doped, $\sim 2–3 \times 10^{18}$ cm^{-3}) DBR contains 28 pairs of AlAs/$Al_{0.12}Ga_{0.88}As$ at the lower part, followed by three pairs of $Al_{0.90}Ga_{0.10}As/Al_{0.12}Ga_{0.88}As$ on top and just below the cavity. Utilizing the high-thermal-conductivity binary compound AlAs facilitates efficient vertical heat transport from the active region through the bottom DBR and therefore reduces the thermal resistance. This is of particular importance in small-aperture VCSELs, which usually suffer from thermal issues more than large-aperture VCSELs.

The active region employs five 4 nm thick $In_{0.10}Ga_{0.90}As$ quantum wells (QWs) separated by 6 nm $Al_{0.37}Ga_{0.63}As$ barriers. Incorporating indium in the QWs results in increased differential gain through strain-induced valence band splitting and enhanced quantum size effects [19]. The top DBR is formed by 23 pairs of p-type (C-doped, $\sim 2–6 \times 10^{18}$ cm^{-3}) $Al_{0.90}Ga_{0.10}As/Al_{0.12}Ga_{0.88}As$. Two 30 nm thick $Al_{0.98}Ga_{0.02}As$ layers were introduced in the top DBR right above the cavity to allow for wet oxidation during device processing and for defining the current and optical aperture. Four additional 30 nm thick AlGaAs oxide layers with 96% Al-content are placed above the two high-Al-content oxide layers to reduce the parasitic oxide capacitance.

B. VCSEL Fabrication

The VCSELs were fabricated through a sequence of standard high-speed VCSEL processing steps including mesa formation, metal contact deposition, wet oxidation, and planarization. The fabrication started by sputter deposition of a Ti/Au ring metal contact on a highly doped GaAs cap layer. Then, VCSEL mesas with 22, 24, 26, and 28 μm diameters were defined by dry etching of the patterned surface using an inductively coupled plasma system with $SiCl_4$/Ar and Cl_2/Ar gas mixtures. The etching was precisely stopped at the desired position above AlAs layers by *in situ* optical etch depth monitoring. After mesa etching, the sample was covered by SiN_x by using plasma-enhanced chemical-vapor deposition to avoid surface oxidation during the wet oxidation process. This step was followed by removal of the SiN_x on the mesa sidewalls by NF_3 plasma etching and definition of the oxide aperture by using selective wet oxidation at 420°C. The oxidation process was monitored by an IR microscope to form small, 2–4 μm aperture, VCSELs with 22 μm diameter mesas for (quasi)-single-mode operation with >1 mW output power. In the next step, a deeper mesa with 50 μm diameter was etched down to a 1 μm thick n-contact layer below the n-DBR using the inductively coupled plasma system and gas mixtures similar to those used for the shallow mesa etch. The larger mesa diameter at the bottom facilitates heat transport from the active region through the bottom DBR. An electron-beam evaporated Ni/Ge/Au contact was then deposited on the highly doped ($\sim 4 \times 10^{18}$ cm^{-3}) contact layer as an n-type contact followed by lift-off and contact annealing at 420°C in an N_2 environment to reduce the contact resistivity. Before VCSEL planarization with benzocyclobutene (BCB), the contact layer under the signal bond pad was etched away to minimize the pad capacitance. The VCSEL fabrication was finished by sputter deposition of a Ti/Au bond pad on the BCB to form a ground–signal–ground contact configuration for device measurement. The completed VCSEL is schematically illustrated in Fig. 1. To boost the output power, slope efficiency, and speed of the VCSELs, the reflectivity of the output coupling DBR was adjusted by shallow inductively coupled plasma etching of the top mesa surface [18] using a $SiCl_4$/Ar gas mixture and 50 W RF power. This step, with ~50 nm etch depth, led to an approximately 40% increase of the maximum output power and the slope efficiency with only a slight increase in threshold current. Having a high launched optical power is essential

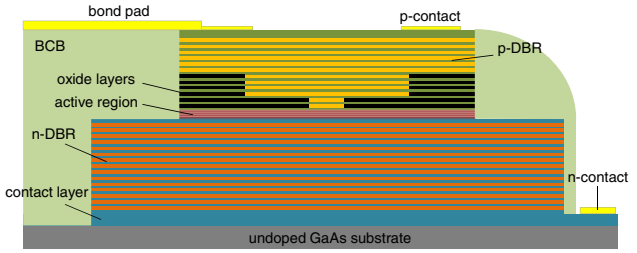

Fig. 1. Cross section view of the fabricated VCSEL.

to compensate for fiber and connector losses for transmission over long fibers.

III. VCSEL Characterization

A. DC Measurements

The light output power–current–voltage (LIV) characteristics of a ~3 μm oxide aperture diameter VCSEL at 20°C after top mirror reflectivity adjustment are presented in Fig. 2. The VCSEL has a threshold current of 0.19 mA, a 44% differential quantum efficiency, and an ~230 Ω differential resistance. The output power measured by a calibrated large-area silicon photodetector is 2 mW at the thermal roll-over current of 5.7 mA. The VCSEL operates primarily in the fundamental mode with a side-mode suppression ratio of 33, 22, and 18 dB at 1, 2, and 2.7 mA, respectively. The corresponding RMS spectral widths ($\Delta\lambda_{\mathrm{rms}}$) are 0.18, 0.21, and 0.29 nm. These values are well below the required $\Delta\lambda_{\mathrm{rms}} = 0.45$ nm for IEEE standards [20] and stay below that for up to 5 mA bias current. The optical emission spectra of the VCSEL at different bias currents are shown in Fig. 3. The optical spectra under modulation do not show any remarkable difference from the presented DC spectra. The reduced VCSEL spectral width directly reduces the effects of chromatic fiber dispersion while it also reduces the effects of modal dispersion, since the quasi-single-mode VCSEL excites a reduced number of fiber modes. This leads to a higher effective fiber bandwidth, which enables a longer transmission distance, assuming no connectors or bends in the fiber causing redistribution of the modes.

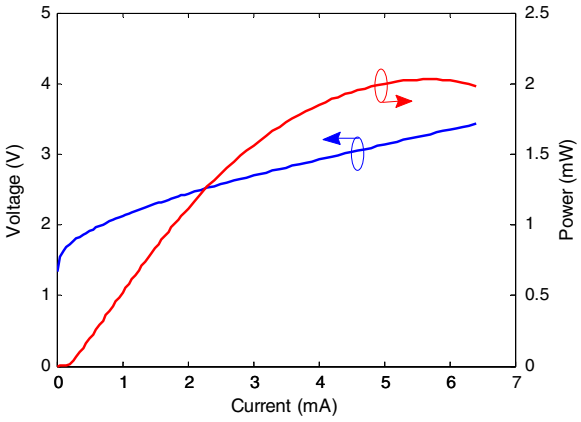

Fig. 2. LIV characteristics of the ~3 μm aperture VCSEL.

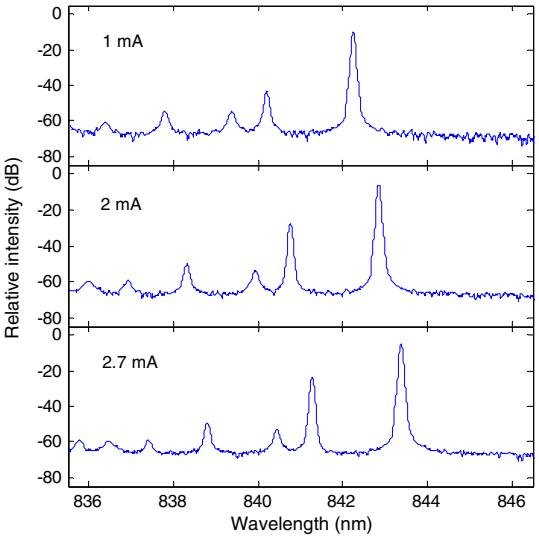

Fig. 3. Optical spectra of the ~3 μm aperture VCSEL at 1, 2, and 2.7 mA.

The DC characteristics suggest that this VCSEL meets the modal properties and power requirements for long-distance MMF transmission. The required output power at modulation current for a 1 km MMF link at a data-rate of ~20 Gbits/s can be estimated to be ~1–2 mW, accounting for 50% coupling loss, 2.2 dB/km fiber loss (for OM4 fiber), 0.5 dB loss per connector, and a −6 dBm receiver sensitivity for error-free detection.

B. AC Characterization

A modulation bandwidth of 23 GHz was already reported for a 7 μm aperture diameter VCSEL with the same epitaxial design and optimized photon lifetime [21]. The frequency response of the ~3 μm aperture VCSEL was measured by using a 65 GHz Anritsu 3797C vector network analyzer and a GaAs 1481 pin photodetector from New Focus with 25 GHz bandwidth and a responsivity of 0.4 A/W at 850 nm. The measured response is then corrected for the frequency responses of the photodetector and the high-speed ground–signal–ground probe. The modulation responses of the VCSEL, depicted in Fig. 4 for different bias currents, show a maximum 3 dB frequency of 21 GHz. The low-frequency roll-off observed in the modulation response, particularly at low bias currents, can be attributed to the effects of spatial hole burning in the active region [22]. A second-order system transfer function derived from the single-mode rate equations, with an additional pole accounting for the effects of electrical parasitics and carrier transport with a cutoff frequency f_p, Eq. (1) [23], is then fitted to the modulation responses in Fig. 4:

$$H(f) = \text{const.} \times \frac{f_r^2}{f_r^2 - f^2 + j(f/2\pi)\gamma} \times \frac{1}{1 + j(f/f_p)}. \quad (1)$$

The transfer function, $H(f)$, is used to extract the relaxation resonance frequency, f_r, and the damping factor, γ, for

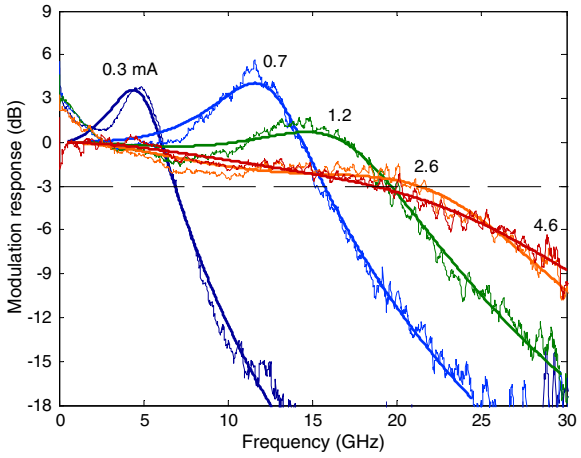

Fig. 4. Modulation response of the VCSEL under test at different bias currents.

each bias current. The damping factor can be written as a function of resonance frequency squared, $\gamma = K \cdot f_r^2 + \gamma_0$, where the K-factor describes the rate at which damping increases with resonance frequency and γ_0 is the damping factor offset [24], which is important at low bias currents where f_r is small. Fig. 5 shows a plot of γ as a function of f_r^2 and the linear fit that determines the K-factor and the damping offset to be 0.17 ns and 6.8 ns^{-1}, respectively. Such a small K-factor yields values exceeding 50 GHz for the damping-limited maximum modulation bandwidth, which can be expressed as $f_{3\,\mathrm{dB,damping}} \approx 2\pi\sqrt{2}/K$ [24]. A small K-factor, and thus small damping, is essential for realizing high-modulation-bandwidth VCSELs. However, a certain amount of damping is needed to prevent excessive ringing and timing jitter. Therefore, there is an optimum amount of damping for a given bit rate.

The D-factor, which describes how fast f_r increases with increasing bias current, I, above the threshold current, I_{th}, $f_r = D \cdot (I - I_{\mathrm{th}})^{1/2}$, is another parameter of importance for the VCSEL dynamics. Achieving high resonance frequencies at low bias currents, and therefore a large D-factor, is desired for high-speed modulation. A large D-factor is also essential for high energy efficiency at high bit rates [14], since a high f_r, and therefore a high modulation bandwidth, can be reached at a lower bias current and voltage. The D-factor can be increased by improving internal quantum efficiency and differential gain and by reducing the cavity volume [24] through proper epitaxial design and small aperture diameters. A large D-factor and high slope efficiency enable high modulation bandwidth and output power at low bias currents, which lead to low power consumption in high-speed, longer distance data transmission.

Fig. 6 presents f_r as a function of $(I - I_{\mathrm{th}})^{1/2}$ for the VCSEL under test, where D is estimated from the fit to the linear part of the curve, before reaching thermal saturation at high bias currents. Large values of $D = 17.3$ GHz/$\mathrm{mA}^{1/2}$ and $f_{r,\max} = 25$ GHz are achieved for this small-aperture VCSEL. The maximum 3 dB bandwidth when only thermal effects are considered [24] is limited to $f_{3\,\mathrm{dB,thermal}} \approx 1.55 \cdot f_{r,\max} = 39$ GHz, which is well above the 3 dB bandwidth of this VCSEL. Therefore, thermal effects are not considered a major bandwidth-limiting factor for this design. The main bandwidth-limitation effect, in fact, was found to be the parasitic electrical elements according to the measured impedance characteristics. This was done by fitting a VCSEL parasitic equivalent-circuit model [25] to the measured S_{11} data. The RC parasitic cutoff frequency, f_{RC}, was then estimated from the parasitic elements. This showed that 11 GHz $< f_{\mathrm{RC}} <$ 18 GHz for bias currents between 0.3 and 5 mA ($f_{\mathrm{RC}} = 16$ GHz at 2.6 mA bias current). Reducing the mirror resistance and improving the carrier transport to the QWs to reduce the diffusion capacitance have recently been shown to increase the VCSEL 3 dB bandwidth to 28 GHz [26]. Although the parasitic cutoff frequency could also be estimated from the fit of the transfer function to the S_{21} data (f_p), the parasitic frequency extracted from S_{11} data is believed to give a more accurate value (f_{RC}). Additionally, S_{11} data provides quantitative values for each parasitic element, which can be useful for improving the epitaxial design.

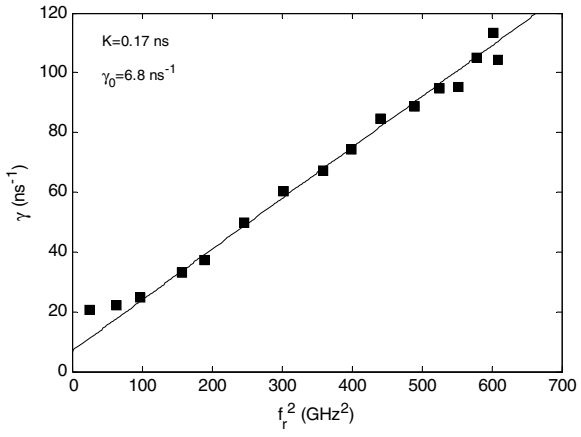

Fig. 5. Damping rate as a function of resonance frequency squared.

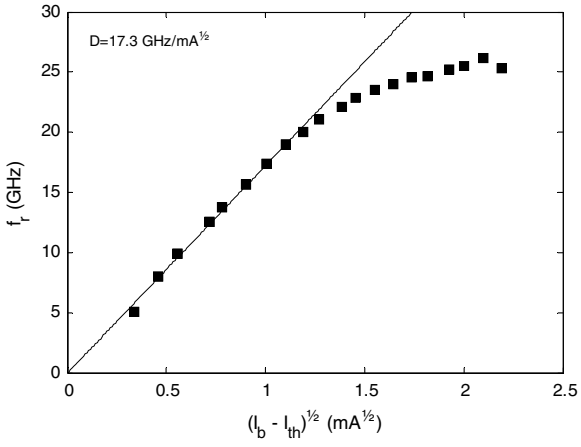

Fig. 6. Resonance frequency as a function of square root of current above threshold.

C. Transmission Experiment

The large signal modulation performance of the quasi-single-mode VCSEL was evaluated at 20°C by recording eye diagrams and BERs for BTB and after 500, 800, and 1100 m transmission on Draka MaxCap-OM4 MMF. The measurement setup for the transmission experiments is shown in Fig. 7.

A non-return-to-zero data pattern with a 2^7–1 bits long pseudorandom binary sequence, generated by an SHF 12103A bit pattern generator, was fed to the VCSEL through a linear SHF 807 amplifier with 24 dB gain in combination with a total of 23 dB attenuation and a 30 GHz SHF 120A bias-T via the ground–signal–ground high-speed probe. The linear amplifier and the attenuators were employed to suppress unwanted microwave reflections resulting from VCSEL impedance mismatch to 50 Ω. The light output was butt-coupled to a 62.5 μm core diameter MMF, which was aligned for ~50% coupling efficiency, before launching to 50 μm core diameter OM4 MMFs. Single fiber spools were used for 500 and 800 m long data transmission, whereas the 1100 m long link was made by connecting 300 and 800 m fiber spools. Two additional 1 m OM4 fiber patch cords, with a flat connector on one end and an angled connector on the other end, were used to adapt the angled ends of the fiber spools to the flat fiber connectors. The fiber was then connected to a JDSU OLA-54 variable optical attenuator to vary the received optical power at the photoreceiver for the BER measurement. The photoreceiver package used for the transmission experiments contains a New Focus 1580 photodiode, with a nominal bandwidth of 12 GHz and a responsivity of 0.4 A/W at 850 nm, and an integrated transimpedance amplifier. The actual response of the photoreceiver showed a 3 dB bandwidth of 10 GHz and a 6 dB cutoff frequency of 14 GHz. The use of an integrated amplifier in the photoreceiver package can effectively reduce the noise level and improve the signal quality by better impedance matching for reduced microwave reflections. However, the photoreceiver available at the time of this experiment has a limited bandwidth, which affects measurements at high bit rates. This limit will be addressed in more detail in the next section.

Another 1 m long OM4 patch cord was used to connect the variable attenuator to the optical input of the photoreceiver, while the output electrical signal was used to record eye diagrams using an Agilent Infiniium DCA-J 86100C 70 GHz digital communications analyzer or to perform BER analysis using an SHF 11100B error analyzer. The VCSEL was biased at 2.7 mA (~38 kA/cm^2), and the peak-to-peak modulation voltage delivered to the VCSEL was ~1.6 V for all transmission measurements. The VCSEL reliability at such high current densities needs to be investigated, even though the small-aperture VCSELs are believed to be able to reliably operate at higher current densities than the large-aperture ones [17]. The VCSEL energy dissipation, defined as dissipated power/bit rate, is 220 fJ/bit for data transmission at 25 Gbits/s. Dissipated power was calculated as $P_{\text{diss}} = \text{IV} - P_{\text{opt}}$, where V and P_{opt} are bias voltage and output power, respectively, at bias current, I. The record VCSEL energy efficiency of 188 fJ/bit was reported for transmission over 600 m at 25 Gbits/s using an ~4 μm oxide aperture quasi-single-mode 850 nm VCSEL [14].

Inverted eyes and results from BER measurements for data rates of 20 and 22 Gbits/s are shown in Figs. 8 and 9, respectively, for BTB transmission and after transmission over 500, 800, and 1100 m of OM4 MMF. Open eyes and error-free operation were achieved for transmission up to 1100 m at both data rates. However, the eyes at 22 Gbits/s for transmission over longer fibers suffer from intersymbol interference (ISI), which limits the transmission distance at data rates exceeding 22 Gbits/s. A power penalty of approximately 2 dB is observed when increasing the transmission distance from BTB to 1100 m, at which the received optical power for BER = 10^{-12} is below −7 dBm at 20 Gbits/s and about −6 dBm at 22 Gbits/s.

A reduction of the required received optical power is observed at 22 Gbits/s when the transmission length is increased from 800 to 1100 m. This can be attributed to a change in the fiber frequency response due to an improved mode power distribution in the fiber when connecting the 300 and 800 m fiber spools. This effect can alter the ISI, and consequently the system performance, and has been previously studied by using an advanced MMF link modeling tool [27]. Despite the reduction of the required received optical power for increasing the fiber length from 800 to

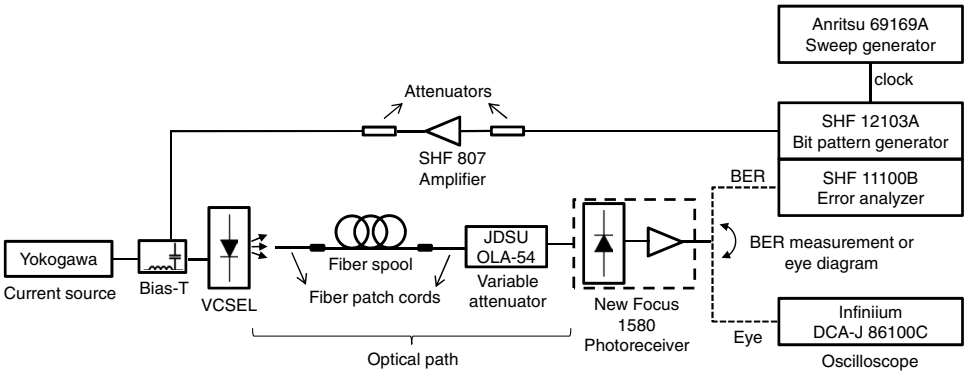

Fig. 7. Measurement setup for transmission experiments.

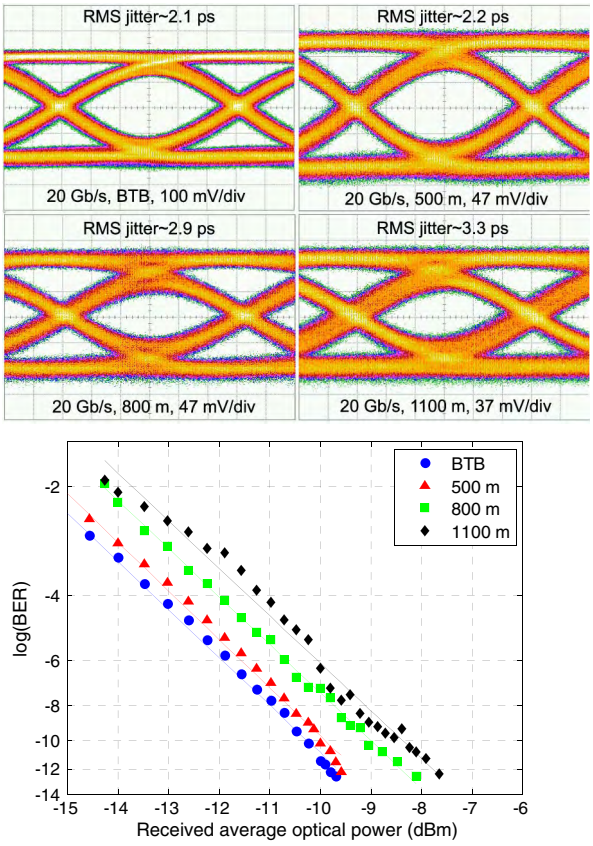

Fig. 8. Eye diagrams and BER measurements for 20 Gbits/s data transmission BTB and over 500, 800, and 1100 m of MMF [15].

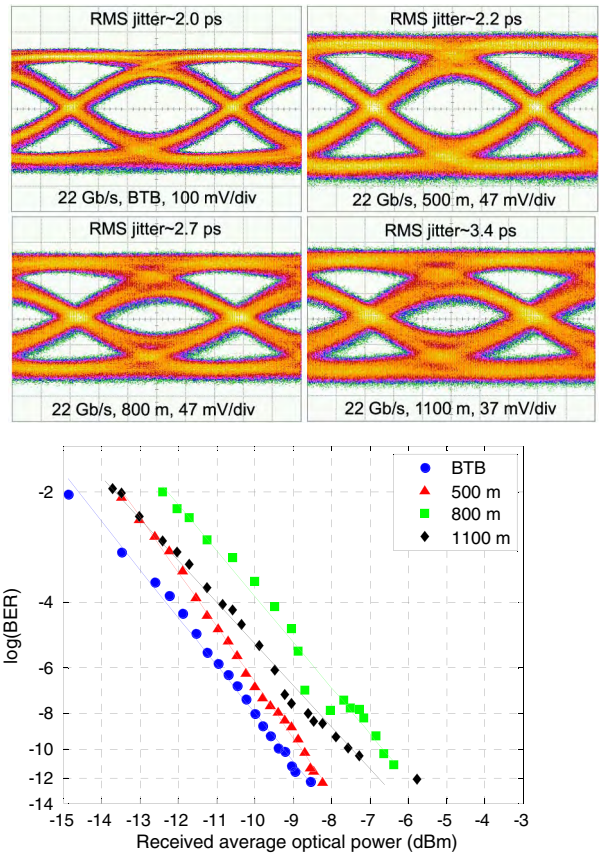

Fig. 9. Eye diagrams and BER measurements for 22 Gbits/s data transmission BTB and over 500, 800, and 1100 m of MMF.

1100 m at 22 Gbits/s, the presented eye diagram for 800 m fiber shows a lower jitter and ISI than the one for 1100 m fiber. This discrepancy may be due to sensitivity of link response to fiber configuration and caused by different fiber arrangements while performing BER and eye diagram measurements for the quasi-single-mode VCSEL. The increased jitter with fiber length for both 20 and 22 Gbits/s bit rates is attributed to the increased effect of fiber dispersion with increased fiber length.

Data transmission at 25 Gbits/s was performed BTB and with 500 and 800 m MMF to find the upper limit of the transmission capacity with the current setup. The results, presented in Fig. 10, indicate that even though error-free transmission is achieved BTB and after 500 m of fiber, a higher laser optical power is needed to meet the receiver sensitivity requirement for the 800 m MMF case. Error-free transmission over longer distances of MMF can also be achieved by improving the system bandwidth (which is limited mainly by the bandwidth of the photoreceiver) for reduced ISI and improved receiver sensitivity at this bit rate.

The increased variance observed in the measured BER data for all bit rates at longer fibers may be related to readjusting the decision point in the eye to compensate for any bias drift during BER measurement. This behavior will be more pronounced at higher bit rates and longer fibers where the link experiences more ISI.

IV. Discussion

To analyze the data transmission results and identify the factors limiting the bit rate and fiber length, theoretical receiver sensitivities at BER $= 10^{-12}$ were calculated for different bit rates and fiber lengths. This calculation was

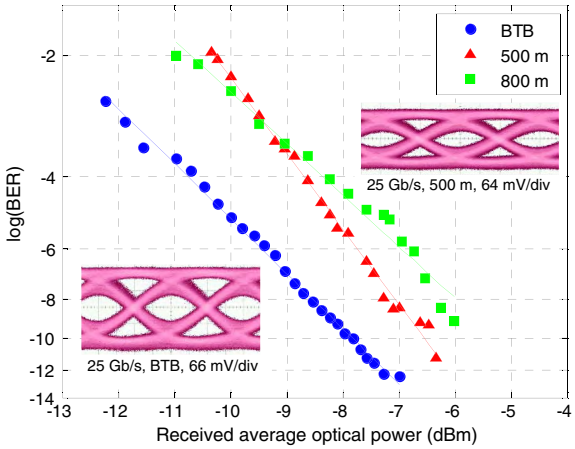

Fig. 10. BER measurements for 25 Gbits/s data transmission BTB and over 500 and 800 m of MMF. The insets show the eye diagrams for BTB and over 500 m data transmission.

performed for the setup used in the previous section for transmission experiments with the 10 GHz bandwidth receiver, as well as for the same setup but with a theoretical 15 GHz bandwidth receiver instead. It is shown below that this bandwidth is theoretically sufficient for 25 Gbits/s data transmission over ~1 km of fiber. The calculations are based on measured frequency responses of the link including a similar VCSEL as reported here along with the 10 GHz photoreceiver and the same MMF. The link S_{21} was measured for the setup with the 10 GHz photoreceiver and all fiber lengths employed in the experiment. The obtained total link bandwidth values were then used to estimate fiber bandwidth for each fiber length. The fiber bandwidths were later used to calculate the total bandwidth of the link while employing a theoretical 15 GHz bandwidth photoreceiver. The 3 dB link bandwidths were extracted from a Gaussian fit to the measured link frequency response and used to estimate rise times for different fiber lengths. The ISI penalty estimated from the rise time values was then used to calculate the receiver sensitivity as a function of bit rate. For the sensitivity calculations, it is assumed that the dominant noise source is thermal noise, which is justified for received power levels below 0 dBm, before shot noise and VCSEL relative intensity noise start to dominate. The noise bandwidth is assumed to be equal to the receiver bandwidth. This model and the assumptions are fully outlined in [28]. In the case of a Gaussian frequency response, the total bandwidth of the system, BW_{tot}, can be estimated from the bandwidth of each component as

$$BW_{tot}^{-2} \approx BW_{rec}^{-2} + BW_{las}^{-2} + BW_{fib}^{-2}, \quad (2)$$

where BW_{rec}, BW_{las}, and BW_{fib} represent receiver, laser, and fiber bandwidths, respectively. Using the known values for BW_{rec} and BW_{las}, the value of BW_{fib} was estimated from Eq. (2) and was later used to approximate the BW_{tot} for the case of the theoretical photoreceiver with 15 GHz bandwidth. This provides an estimate of system performance when using a photoreceiver with higher bandwidth. Although the real systems may not have a Gaussian response, this model simplifies the overall system behavior with an acceptable accuracy. Sensitivities at BER $= 10^{-12}$ were calculated for a range of bit rates for BTB and different fiber lengths. This calculation was performed for the 10 GHz bandwidth photoreceiver employed in the experiment and also for a theoretical 15 GHz bandwidth photoreceiver to investigate the effect of limited receiver bandwidth on the performance. Calculated and measured sensitivity values at 20, 22, and 25 Gbits/s are summarized in Table I, where it is evident that the difference between calculated and measured values are less than 0.5 dB for all cases, except the case of 800 m at 20 Gbits/s. The lower calculated sensitivity for the 1100 m fiber case, compared to the 800 m case, arises from the higher measured system bandwidth for the 1100 m case, which is in agreement with the 22 Gbits/s BER measurement shown in the previous section. The calculated sensitivities using the theoretical 15 GHz photoreceiver are also given in Table I for different fiber lengths at 20, 22, and 25 Gbits/s.

TABLE I
MEASURED AND CALCULATED SENSITIVITY VALUES[a] AT BER $= 10^{-12}$

		BTB	500 m	800 m	1.1 km
10 GHz real receiver	20G meas.	−9.6	−9.3	−8.4	−7.7
	20G calc.	−9.7	−8.9	−7.2	−7.8
	22G meas.	−8.6	−8.2	−6.0	−6.7
	22G calc.	−8.8	−7.8	−5.6	−6.4
	25G meas.	−7.2	−6.1	—	—
	25G calc.	−7.3	−5.9	−2.2	−3.6
15 GHz theoretical receiver	20G calc.	−10.7	−9.9	−8.3	−8.8
	22G calc.	−10.2	−9.3	−7.2	−7.9
	25G calc.	−9.4	−8.2	−5.4	−6.4

[a]Sensitivity values are given in dBm.

As expressed in the table, utilizing a 15 GHz receiver improves sensitivities by 1–2 dB for all bit rates. This is a result of reduced ISI. It is also evident that the calculated receiver sensitivities with the 15 GHz receiver at 25 Gbits/s are almost equal to, or better than, the case with the 10 GHz receiver at 22 Gbits/s. This indicates that by employing a 15 GHz receiver one can achieve data transmission over ~1 km of MMF at 25 Gbits/s using the quasi-single-mode VCSEL and OM4 fiber.

The calculations for a 2 km link showed that a photoreceiver with higher than 15 GHz bandwidth is required in order to achieve a sensitivity of < -6 dBm for 20 Gbits/s data transmission over 2 km of MMF. To increase the reach at high bit rates (25 Gbits/s in this case), the VCSEL output power should be high enough to overcome the connector and fiber losses and effects of fiber dispersion to reach the required receiver sensitivity levels for the error-free detection. Moreover, VCSELs with narrower spectral width (smaller number of transverse modes) are favorable to reduce the effects of chromatic and modal dispersion in the fiber. This renders a higher effective bandwidth for the fiber, which can alter the overall system performance, in particular when it is not limited by the receiver bandwidth. However, one should also consider larger modal noise in the links employing MMFs and higher coherence, narrow-spectral-width VCSELs resulting from interference between fiber modes and mode selective loss in the link [29].

V. CONCLUSION

High-speed, small-aperture VCSELs for extended-reach data communication at high bit rates were presented. The small oxide aperture (~3 μm) and the reduced top DBR reflectivity led to a narrow spectral width (0.29 nm) for high fiber bandwidth, high slope efficiency for efficient modulation, a high output power (2 mW) to overcome power loss during transmission over long lengths of fiber, and a high modulation bandwidth (21 GHz) for transmission at high bit rates. This enabled error-free data transmission over more than 1 km of OM4 MMF at bit rates exceeding 20 Gbits/s. Data transmission at 20, 22, and 25 Gbits/s over different fiber lengths and a corresponding theoretical

analysis revealed that the achievable bit rate at long transmission distances was limited by the bandwidth of the photoreceiver used in the experiment. Calculations with a theoretical photoreceiver bandwidth of 15 GHz showed a significant improvement of the receiver sensitivity due to reduced ISI, which should allow for 25 Gbits/s data transmission over 1 km of MMF using these VCSELs. Employing quasi-single-mode VCSELs with even higher output power and narrower spectral width will enable transmission over even longer MMFs.

Acknowledgments

The authors would like to thank IQE Europe Ltd. for providing the epitaxial growth.

References

[1] C. F. Lam, H. Liu, B. Koley, X. Zhao, V. Kamalov, and V. Gill, "Fiber optic communication technologies: what's needed for datacenter network operations," *IEEE Commun. Mag.*, vol. 48, no. 7, pp. 32–39, July 2010.

[2] H. Liu, C. F. Lam, and C. Johnson, "Scaling optical interconnects in datacenter networks: opportunities and challenges for WDM," in *18th IEEE Symp. High Performance Interconnects (HOTI)*, Mountain View, CA, 2010, pp. 113–116.

[3] A. Larsson, "Advances in VCSELs for communication and sensing," *IEEE J. Sel. Top. Quantum Electron.*, vol. 17, no. 6, pp. 1552–1567, Dec. 2011.

[4] M. A. Taubenblatt, "Optical interconnects for high-performance computing," *J. Lightwave Technol.*, vol. 30, no. 4, pp. 448–457, Feb. 2012.

[5] J. B. Schlager, M. J. Hackert, P. Pepejugoski, and J. Gwinn, "Measurements for enhanced bandwidth performance over 62.5 μm multimode fiber in short-wavelength local area networks," *J. Lightwave Technol.*, vol. 21, no. 5, pp. 1276–1285, May 2003.

[6] A. Gholami, D. Molin, and P. Sillard, "Compensation of chromatic dispersion by modal dispersion in MMF- and VCSEL-based gigabit Ethernet transmissions," *IEEE Photon. Technol. Lett.*, vol. 21, no. 10, pp. 645–647, June 2009.

[7] R. E. Freund, C.-A. Bunge, N. N. Ledentsov, D. Molin, and C. Caspar, "High-speed transmission in multimode fibers," *J. Lightwave Technol.*, vol. 28, no. 4, pp. 569–586, Feb. 2010.

[8] P. Pepeljugoski, D. Kuchta, Y. Kwark, P. Pleunis, and G. Kuyt, "15.6 Gb/s transmission over 1 km of next generation multimode fiber," *IEEE Photon. Technol. Lett.*, vol. 14, no. 5, pp. 717–719, May 2002.

[9] P. Westbergh, R. Safaisini, E. Haglund, J. S. Gustavsson, A. Larsson, M. Geen, R. Lawrence, and A. Joel, "High-speed oxide confined 850 nm VCSELs operating error-free at 40 Gbit/s up to 85°C," *IEEE Photon. Technol. Lett.*, vol. 25, no. 8, pp. 768–771, Apr. 2013.

[10] E. Haglund, Å. Haglund, P. Westbergh, J. S. Gustavsson, B. Kögel, and A. Larsson, "25 Gbit/s transmission over 500 m multimode fibre using 850 nm VCSEL with integrated mode filter," *Electron. Lett.*, vol. 48, no. 9, pp. 517–518, Apr. 2012.

[11] J. A. Lott, A. S. Payusov, S. A. Blokhin, P. Moser, and D. Bimberg, "Arrays of 850 nm photodiodes and vertical cavity surface emitting lasers for 25–40 Gbit/s optical interconnects," *Phys. Status Solidi C*, vol. 9, no 2, pp. 290–293, 2012.

[12] P. Moser, J. A. Lott, P. Wolf, G. Larisch, H. Li, N. N. Ledentsov, and D. Bimberg, "56 fJ dissipated energy per bit of oxide-confined 850 nm VCSELs operating at 25 Gbit/s," *Electron. Lett.*, vol. 48, no. 20, pp. 1292–1294, Sept. 2012.

[13] G. Fiol, J. A. Lott, N. N. Ledentsov, and D. Bimberg, "Multimode optical fibre communication at 25 Gbit/s over 300 m with small spectral-width 850 nm VCSELs," *Electron. Lett.*, vol. 47, no. 14, pp. 810–811, July 2011.

[14] P. Moser, J. A. Lott, P. Wolf, G. Larisch, A. Payusov, N. Ledentsov, and D. Bimberg, "Energy-efficient oxide-confined 850 nm VCSELs for long distance multimode fiber optical interconnects," *IEEE J. Sel. Top. Quantum Electron.*, vol. 19, no. 2, 7900406, 2013.

[15] R. Safaisini, K. Szczerba, E. Haglund, P. Westbergh, J. S. Gustavsson, A. Larsson, and P. A. Andrekson, "20 Gbit/s error-free operation of 850 nm oxide-confined VCSELs beyond 1 km of multimode fibre," *Electron. Lett.*, vol. 48, no. 19, pp. 1225–1227, Sept. 2012.

[16] G. Giaretta, R. Michalzik, and A. J. Ritger, "Long distance (2.8 km), short wavelength (0.85 μm) data transmission at 10 Gb/ sec over new generation high bandwidth multimode fiber," in *Conf. Lasers and Electro-Optics (CLEO)*, San Francisco, CA, 2000, pp. 678–679.

[17] B. M. Hawkins, R. A. Hawthorne, J. K. Guenter, J. A. Tatum, and J. R. Biard, "Reliability of various size oxide aperture VCSELs," in *Proc. 52nd Electronic Components and Technology Conf.*, San Diego, CA, 2002, pp. 540–550.

[18] P. Westbergh, J. S. Gustavsson, B. Kögel, Å. Haglund, and A. Larsson, "Impact of photon lifetime on high-speed VCSEL performance," *IEEE J. Sel. Top. Quantum Electron.*, vol. 17, no. 6, pp. 1603–1613, Dec. 2011.

[19] S. B. Healy, E. P. O'Reilly, J. S. Gustavsson, P. Westbergh, Å. Haglund, A. Larsson, and A. Joel, "Active region design for high-speed 850 nm VCSELs," *IEEE J. Quantum Electron.*, vol. 46, no. 4, pp. 506–512, Apr. 2010.

[20] "IEEE Standard for Information Technology—Telecommunications and Information Exchange Between Systems—Local and Metropolitan Area Networks—Specific Requirements Part 3: Carrier Sense Multiple Access With Collision Detection (CSMA/CD) Access Method and Physical Layer Specifications—Section Four," (Revision of IEEE Standard 802.3-2005), pp. 1–586, Dec. 2008.

[21] P. Westbergh, J. S. Gustavsson, B. Kögel, Å. Haglund, A. Larsson, and A. Joel, "Speed enhancement of VCSELs by photon lifetime reduction," *Electron. Lett.*, vol. 46, no. 13, pp. 938–940, June 2010.

[22] J. S. Gustavsson, A. Haglund, J. Bengtsson, P. Modh, and A. Larsson, "Dynamic behavior of fundamental-mode stabilized VCSELs using shallow surface relief," *IEEE J. Quantum Electron.*, vol. 40, no. 6, pp. 607–619, June 2004.

[23] O. Kjebon, R. Schatz, S. Lourdudoss, S. Nilsson, and B. Stalnacke, "Modulation response measurements and evaluation of MQW InGaAsP lasers of various designs," *Proc. SPIE*, vol. 2684, pp. 138–152, 1996.

[24] L. A. Coldren, S. W. Corzine, and M. L. Mašanović, *Diode Lasers and Photonic Integrated Circuits*, 2nd ed. New Jersey: Wiley, 2012.

[25] Y. Ou, J. S. Gustavsson, P. Westbergh, Å. Haglund, A. Larsson, and A. Joel, "Impedance characteristics and parasitic speed limitations of high speed 850 nm VCSELs," *IEEE Photon. Technol. Lett.*, vol. 21, no. 24, pp. 1840–1842, Dec. 2009.

[26] P. Westbergh, R. Safaisini, E. Haglund, B. Kögel, J. S. Gustavsson, A. Larsson, M. Geen, R. Lawrence, and A. Joel,

"High-speed 850 nm VCSELs with 28 GHz modulation bandwidth operating error-free up to 44 Gbit/s," *Electron. Lett.*, vol. 48, no. 18, pp. 1145–1147, Aug. 2012.

[27] P. Pepeljugoski, S. E. Golowich, A. J. Ritger, P. Kolesar, and A. Risteski, "Modeling and simulation of next-generation multimode fiber links," *J. Lightwave Technol.*, vol. 21, no. 5, pp. 1242–1255, May 2003.

[28] K. Szczerba, P. Westbergh, J. Karout, J. Gustavsson, Å. Haglund, M. Karlsson, P. Andrekson, E. Agrell, and A. Larsson, "4-PAM for high-speed short-range optical communications," *J. Opt. Commun. Netw.*, vol. 4, no. 11, pp. 885–894, Nov. 2012.

[29] D. M. Kuchta and C. J. Mahon, "Mode selective loss penalties in VCSEL optical fiber transmission links," *IEEE Photon. Technol. Lett.*, vol. 6, no. 2, pp. 288–290, 1994.

Rashid Safaisini received the B.S. and M.S. degrees in Electrical Engineering from Shahid Beheshti University and Amirkabir University of Technology (Tehran Polytechnic), Tehran, Iran, in 2003 and 2006, respectively. He then joined Colorado State University in Fort Collins, Colorado, USA, and received the Ph.D. degree in Electrical Engineering in 2011. His main research topics were vertical-cavity surface-emitting laser (VCSEL) dynamics, high-power high-speed VCSEL arrays, and thermal management of VCSELs. He is currently a postdoctoral researcher in the Photonics Laboratory, Department of Microtechnology and Nanoscience, Chalmers University of Technology, Göteborg, Sweden. His current research interests include high-speed VCSELs for data communications and optical interconnects.

Krzysztof Szczerba received his M.Sc. degree in Telecommunications from the Technical University of Denmark, Lyngby, Denmark, and his M.Sc. degree in Electronics and Telecommunications from the Technical University of Lodz, Poland, both in 2008. In 2008, he worked at the Technical University of Denmark, DTU Fotonik, Department of Photonics Engineering as a research assistant. In 2009, he joined the Chalmers University of Technology, Department of Microtechnology and Nanoscience, in Göteborg, Sweden, where he is currently working toward a Ph.D. degree in optical communications. His research interests are focused on modulation formats for short-range optical links for data communication applications.

Petter Westbergh received his M.Sc. degree in Engineering Physics and his Ph.D. degree in Microtechnology and Nanoscience from Chalmers University of Technology, Göteborg, Sweden, in 2007 and 2011, respectively. His thesis focused on the design, fabrication, and characterization of high-speed 850 nm vertical-cavity surface-emitting lasers (VCSELs) intended for application in short-reach communication networks. He is currently continuing his work on improving the performance of high-speed VCSELs with the Department of Microtechnology and Nanoscience at Chalmers University of Technology.

Erik Haglund received his B.Sc. and M.Sc. in Engineering Physics from Chalmers University of Technology, Göteborg, Sweden, in 2007 and 2010, respectively. Since 2010 he has been working toward a Ph.D. in optoelectronics at the Photonics Laboratory at Chalmers University of Technology. His main research interests are fabrication and characterization of high-speed GaAs-based vertical-cavity surface-emitting lasers (VCSELs) and surface structures for spectral engineering of VCSELs.

Benjamin Kögel was born in Herzberg, Germany, in May 1979. He received the Dipl.-Ing. degree in electrical engineering and the Dr.-Ing. degree from Technische Universität Darmstadt, Darmstadt, Germany, in 2003 and 2009, respectively. His thesis includes microelectromechanical systems (MEMS) tunable VCSELs and their applications in sensor systems. From 2009 to 2012 he was a postdoctoral researcher at the Department of Microtechnology and Nanoscience, Chalmers University of Technology, Göteborg, Sweden, where he was working on high-speed and tunable short-wavelength VCSELs. Since 2012 he has been a manager for VCSEL engineering at Vertilas GmbH in Garching, Germany.

Johan S. Gustavsson received his M.Sc. degree in Electrical Engineering and his Ph.D. degree in Photonics from the Chalmers University of Technology, Göteborg, Sweden, in 1998 and 2003, respectively. His main research topics were mode dynamics and noise in VCSELs. Since 2003 he has been a researcher at the Photonics Laboratory, Department of Microtechnology and Nanoscience, Chalmers University of Technology, with an Assistant Professor position during 2004–2008 and an Associate Professor position in 2011. In September–October 2009, he was a visiting scientist at CNR Polytechnico, Turin, Italy. He has authored or co-authored more than 130 scientific journal and conference papers, and his research has been focused on semiconductor lasers for short- to medium-reach communication, and sensing applications. This has included surface relief techniques for mode and polarization control in VCSELs, 1.3 μm InGaAs VCSELs/GaInNAs ridge waveguide lasers for access networks, 2.3–3.5 μm GaSb VCSELs for CO, CO_2, and NH_3 sensing, and tunable VCSELs via moveable mirror for reconfigurable optical interconnects. He is currently working on 40 Gbits/s 850 nm VCSELs for next-generation datacom links, blue/green GaN VCSELs, high-contrast gratings as feedback elements in microcavity lasers, and heterogeneous integration of III/V-based VCSEL material on Si-platforms.

Magnus Karlsson received his Ph.D. in Electromagnetic Field Theory in 1994 from Chalmers University of Technology, Göteborg, Sweden. The title of his Ph.D. thesis was "Nonlinear propagation of optical pulses and beams." Since 1995, he has been with the Photonics Laboratory at Chalmers, first as an Assistant Professor and since 2003 as a Professor in Photonics. He has authored or co-authored more than 190 scientific journal and conference contributions, served as guest editor for the *Journal of Lightwave Technology*, and is currently an associate editor of *Optics Express*. He has served in the technical committees for the Optical Fiber Communication Conference (OFC) (2009 as subcommittee chair) and the Asia Communications and Photonics Conference (ACP, formerly APOC). His research has been devoted to a variety of aspects of fiber optic communication systems, in particular transmission effects, such as fiber nonlinearities and polarization effects, but also applied issues, such as high-capacity data transmission and all-optical switching. Currently he is devoted to parametric amplification, multilevel modulation formats, and coherent transmission in optical fibers.

Peter Andrekson received his Ph.D. from Chalmers University of Technology, Sweden, in 1988. After about three years with AT&T Bell Laboratories, Murray Hill, NJ, USA, during 1989–1992, he returned to Chalmers, where he is now a Full Professor in the Department of Microtechnology and Nanoscience. He was Director of Research at Cenix Inc. in Allentown, PA, USA, during 2000–2003 and with the newly established Center for Optical Technologies at Lehigh University, Bethlehem, PA, USA, during 2003–2004. His research interests include nearly all aspects of fiber communications, such as optical amplifiers, nonlinear pulse propagation, all-optical functionalities, and very high-capacity transmission. He is a co-founder of the optical test and measurement company Picosolve Inc., now part of EXFO; he is a Director of EXFO Sweden AB. Prof. Andrekson is a Fellow of the Optical Society of America and a Fellow of the IEEE. He is the author of about 350 scientific publications and conference papers in the area of optical communications, among

which 80 were invited papers at leading international conferences and journals, including two tutorials at the Optical Fiber Communication Conference (OFC) in 2004 and 2011. He is an elected member of the Board of Governors for the IEEE Photonics Society and is serving or has served on several technical program committees, including OFC and ECOC, and as an international project and candidate evaluator, and has also twice served as an expert for the evaluation of the Nobel Prize in Physics. He was an associate editor for *IEEE Photonics Technology Letters* during 2003–2007. In 1993, he was awarded a prize from the Swedish government research committee for outstanding work performed by young scientists, and in 2000 he was awarded the Telenor Nordic research award for his contribution to optical technologies.

Anders Larsson received the M.Sc. and Ph.D. degrees in electrical engineering from Chalmers University of Technology, Göteborg, Sweden, in 1982 and 1987, respectively. In 1991, he joined the faculty at Chalmers University of Technology where he was promoted to Professor in 1994. From 1984 to 1985 he was with the Department of Applied Physics, California Institute of Technology, and from 1988 to 1991 with the Jet Propulsion Laboratory, both at Pasadena, CA, USA. He has been a guest professor at Ulm University, Germany; at the Optical Science Center, University of Arizona, Tucson, AZ, USA; at Osaka University, Japan; and at the Institute of Semiconductors, Chinese Academy of Sciences, China. He co-organized the IEEE Semiconductor Laser Workshop 2004; organized the European Semiconductor Laser Workshop 2004; was a co-program chair for the European Conference on Optical Communication 2004; and was the program and general chair for the IEEE International Semiconductor Laser Conference in 2006 and 2008, respectively. He is an associate editor for IEEE/OSA *Journal of Lightwave Technology*. His scientific background is in the areas of optoelectronic materials and devices for optical communication, information processing, and sensing. Currently, his research is focused on VCSELs and III-nitride emitters. He has published close to 500 scientific journal and conference papers and 2 book chapters. He is a Fellow of the European Optical Society and a Senior Member of IEEE. In 2012 he received the HP Labs Research Innovation Award.